

Some Constraints on Strength and Rheology of the Plattengneiss Shear Zone (Koraln - Austroalpine)

By Veronika TENCZER* & Kurt STÜWE*

with 4 figures

Angenommen am 21. Juni 1999

Zusammenfassung: Überlegungen zur Festigkeit und Rheologie der Plattengneiss Scherzone (Koraln – Ostalpin). – Die Interpretation des rheologischen Verhaltens des Plattengneisses während der Eoalpidischen Deformationsgeschichte wird durch zwei strukturelle Beobachtungen unterstützt. Die erste Beobachtung betrifft das relative Verformungsverhalten von Porphyroblasten und –klasten, mit unterschiedlichem rheologischen Verhalten zueinander während der Deformation. Die zweite Beobachtung betrifft die Dekompressionsreaktion von Muskovit zu Biotit. In dieser Arbeit konzentrieren wir uns auf die erste Beobachtung. Wir zeigen die rheologischen Beziehungen zwischen rigiden Objekten in weicherer Matrix und die Rolle, welche die rheologischen Unterschiede für die Berechnung der Parameter von exponentiellen Fließgesetzen spielt. Als Anhaltspunkt und Obergrenze berechnen wir die Bedingungen, unter denen sich das rheologische Verhalten zwischen Quarz und Feldspat umkehrt, d.h. unter welchen Bedingungen Quarz härter reagiert als Feldspat. Eine Umkehr in der Festigkeit zwischen diesen beiden Phasen ist nur dann möglich, wenn die Exponenten des Potenzgesetzes für beide Minerale sehr unterschiedliche Werte annehmen. Zum Beispiel, ist es für die experimentell bestimmten Werte für Aktivierungsenergie von Albit möglich, daß Albit weicher als Quarz ist, wenn der Exponent des Potenzgesetzes in einem Bereich von -1.09 bis 25.14 liegt, bei Verformungsraten von 10^{-13} [s^{-1}] bis 10^{-16} [s^{-1}] und Temperaturen von $800^{\circ}C$.

Summary: Two observations commonly made in the Plattengneiss rocks may potentially be interpreted in terms of the rheology of this shear zone during its Eoalpine deformation history. First, a variety of rigid objects of different composition occur in a weaker matrix with different rheological behaviour during deformation. Second, the decompression reaction of muscovite to biotite is preferentially developed in pressure shadows around garnets. Here we explore the rheological relationship between matrix and included objects. We show the role that differences in strength between different mineral phases play for the flow of ductile deforming rocks of the Plattengneiss shear zone. We calculate the conditions at which quartz and feldspar reverse their rheological behaviour as an upper limit. The strength reversal between the two phases can only occur if the stress exponents of quartz and feldspar have considerably different values. The differences in activation energy and pre exponential constant of the flow law play a subordinate role. For example, the experimentally derived activation energy of albite allows it to be softer than quartz if the stress exponent is between -1.09 and 25.14 at reasonable strain rates of 10^{-13} [s^{-1}] to 10^{-16} [s^{-1}] and temperatures of $800^{\circ}C$.

1. Introduction

The stresses during continental deformation are one of the worst constrained parameters of mountain building processes. In the seventies some studies considered such stresses high enough to be responsible for the formation of high pressure metamorphic parageneses at shallow crustal levels (RUTLAND 1965, ERNST 1971). In contrast, experimental studies in the seventies and eighties have shown that crustal minerals can only sustain maximum stresses of the order of few tens of MPa at geologically relevant strain rates and mid crustal temperatures (BRACE & KOHLSTEDT 1980, SHELTON & TULLIS 1981). However, such experiments are subject to extrapolations for many orders of magnitude to be applicable to geological processes and are therefore of limited value. Similarly piezometric methods are often of limited value because of the large number of assumptions necessary to use these

methods. Because of this, a number of recent studies constrained stresses using new methods, for example, crustal scale heat budget calculations or petrological methods applied to stress calculations (MOLNAR & ENGLAND 1990, MANCKTELOW 1993, 1995, STÜWE 1998, SONDER & ENGLAND 1986, MOLNAR & LYON-CAEN 1989). A project recently funded by the FWF at the university of Graz is investigating the magnitude of stresses using an integrated structural and petrological approach. The project focuses on the stresses that prevailed during deformation of one of the largest shear zones of the Alps, the Plattengneiss. Here we present a progress report on this project.

2. Background Geology of the Plattengneiss

The Plattengneiss shear zone is the structurally highest part of the Koralm complex and is part of the Austro-Alpine nappe complex. This major mylonite zone (up to 700 m thickness) consists of predominantly metapelitic sediments and was synchronously metamorphosed and deformed in the Cretaceous (THÖNI & JAGOUTZ 1992). Eoalpine metamorphism reached peak conditions of amphibolite to eclogite grade in the south (MILLER & FRANK 1983, MILLER 1990) and decreases continuously northwards (THÖNI & JAGOUTZ 1992, THÖNI & MILLER 1996). Structural investigations also indicate a change in strain-intensity from north to south along this huge mylonitic sheet (KROHE 1987, FLÖTTMANN & al. 1986). The northwards drop in peak pressure is in contrast to peak metamorphic temperatures which are relatively similar throughout the whole north-south section (NEUBAUER & al. 1995, STÜWE 1998).

3. The Problem

There are two basic observations which are common to large parts of the Plattengneiss shear zone and which both may potentially be interpreted with respect to their information on the stresses during deformation. Firstly, the rocks contain large accumulations of rheologically differently behaving spherical objects relative to the matrix during deformation, e.g. feldspar porphyroclasts with variable chemistry and spherical quartz aggregates. Most minerals show features of dynamic deformation as shown in (Fig.1). Secondly, the rocks contain biotite as a down-pressure reaction product from muscovite. This biotite is located preferentially in the pressure shadows behind garnet.

The fact that biotite grows in pressure shadows is not trivial to interpret but has also potential relevance for the interpretation of stresses. Biotite is a common retrograde reaction product in pelitic rocks. In rocks with the peak paragenesis garnet-muscovite-quartz, it is a typical reaction product from muscovite and is indicative of decompression of the rocks from the metamorphic peak. Traditionally this decompression reaction has been interpreted as being indicative of the exhumation of the rocks to the Earth's surface. However, in the Plattengneiss rocks, biotite grows preferentially in pressure shadows around garnet, while muscovite in the matrix is often unaffected by consumption by biotite. Thus, it is possible, that the growth of biotite is not related to the exhumation (decrease of the lithostatic stress) but to a local decrease of the mean stress in the pressure shadow behind the garnet (Fig.2a). On (Fig.2b) we have contoured a petrogenetic pseudosection for the bulk composition of the Plattengneiss for volumetric proportions of minerals. It may be seen that for every 100 MPa of decompression at the temperatures relevant for peak conditions of the Plattengneiss (path A-A' on Fig.2b) the volumetric proportions of biotite increases by about 5 Vol% on the expense of about 2 Vol% muscovite and 1 Vol% garnet. Mean stress changes in the order of 100 MPa as a function of non-lithostatic stress changes are not unrealistic and the interpretation of this observa-

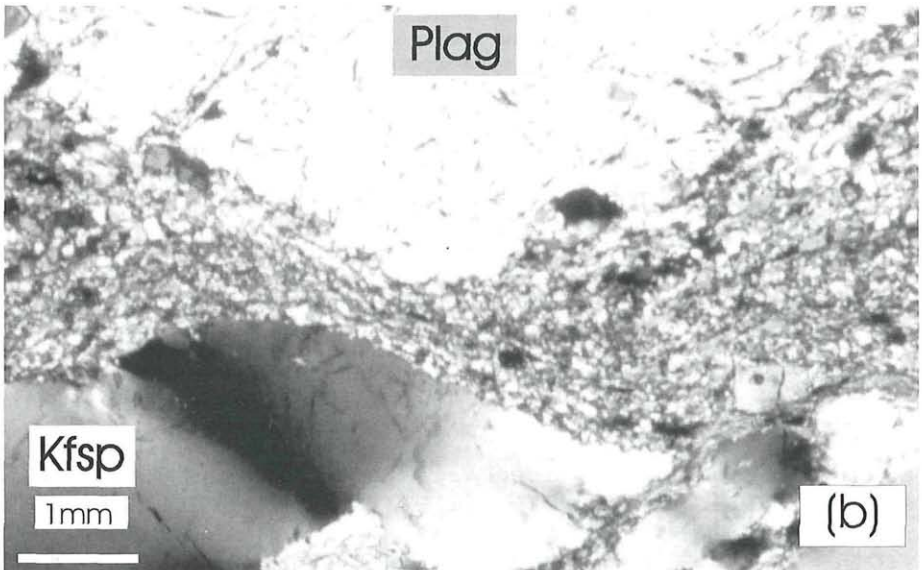
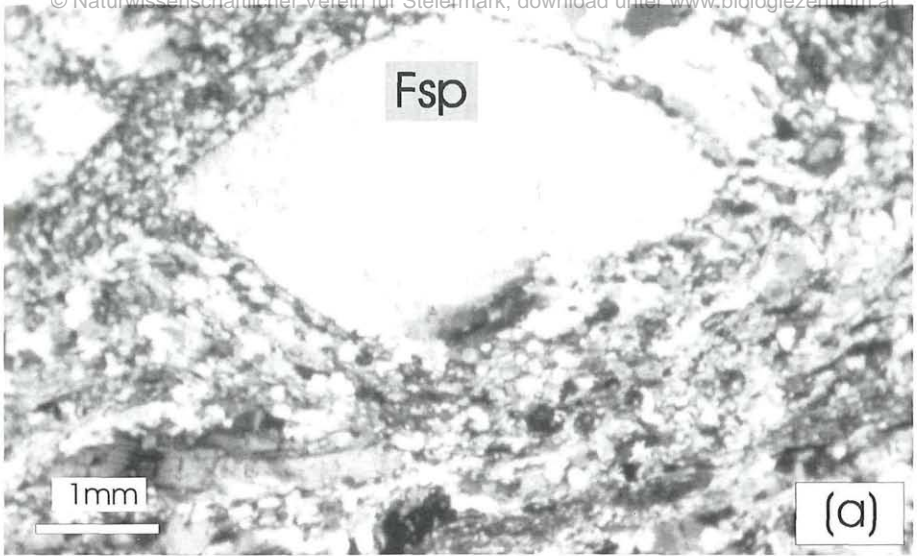


Fig. 1: Photomicrographs of dynamically recrystallised objects of feldspar in a matrix consisting of feldspar, quartz and mica out of the Plattengneiss. (a) Porphyroclast of K-feldspar showing a core-mantle texture with subgrains in a matrix of quartz, plagioclase and mica. (b) Thin section showing dynamically-recrystallised K-feldspar and plagioclase with subgrains and undulous extinction.

Dünnschliff-Fotos von dynamisch rekristallisierten Feldspatklüsten in einer Matrix, die aus Feldspat, Quarz und Glimmer besteht, aus dem Plattengneiss (a) Kalifeldspat-Porphyroklast, der eine Kern-Mantel-Textur zeigt, mit Subkornbildung in einer Matrix aus Quarz, Plagioklas und Hellglimmer. (b) Dünnschliff mit dynamisch rekristallisiertem Kalifeldspat und Plagioklas mit Subkörnern und undulösem Auslöschchen.

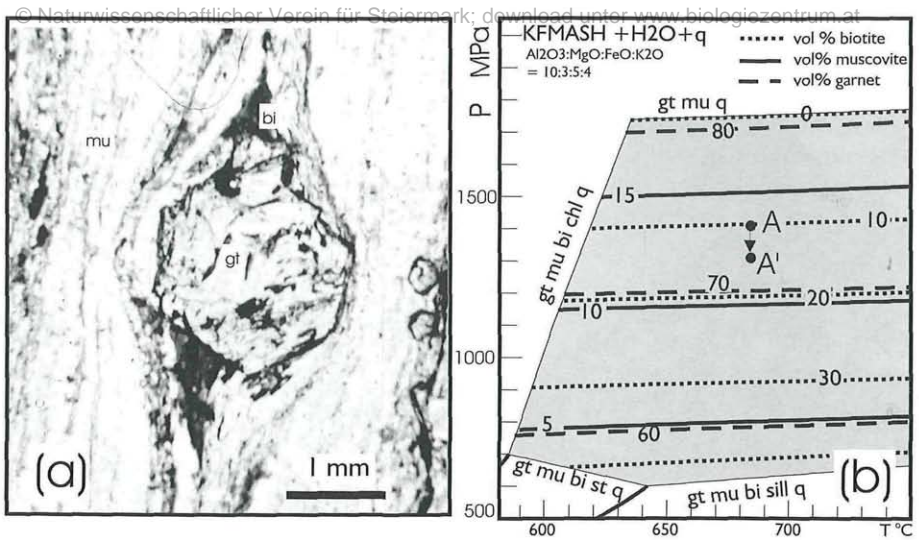


Fig. 2: Decompression reactions in the Plattengneiss and its interpretation. (a) Photomicrograph of a garnet (gt) with newly-formed biotite (bi) growing in its pressure shadow. The matrix is made up of muscovite (mu) and quartz. (b) Petrogenetic pseudosection in the system $K_2O-FeO-MgO-Al_2O_3-SiO_2-H_2O$ for rocks of the bulk composition of the Plattengneiss in the PT range of interest. The chosen bulk composition is that of STÜWE & POWELL (1995). The shaded field is the trivariant field garnet-muscovite-biotite-quartz. It is bound at lower temperature and lower pressures by the indicated divariant parageneses and at higher pressures by the indicated quadrivariant paragenesis. In the relevant trivariant field, the reaction of garnet plus muscovite to biotite is practically only pressure dependent.

Dekompressionsreaktionen im Plattengneiss und ihre Interpretation. (a) Dünnschliff eines Granats (gt) mit neugebildetem Biotit (bi), der im Druckschatten wächst. Die Matrix besteht aus Muskovit (mu) und Quarz. (b) Petrogenetischer Pseudoschnitt im System $K_2O-FeO-MgO-Al_2O_3-SiO_2-H_2O$ für Gesteine mit der Gesamtzusammensetzung des Plattengneisses im relevanten PT-Feld. Die gewählte Gesamtzusammensetzung basiert auf STÜWE & POWELL (1995). Der schattierte Bereich ist das trivariante Feld von Granat-Muskovit-Biotit-Quarz. Es wird begrenzt bei abfallender Temperatur und geringeren Drucken durch die eingezeichneten divarianten Paragenesen und bei höheren Drucken durch die engetragenen quadrivarianten Paragenesen. Im relevanten trivarianten Feld ist die Reaktion von Granat plus Muskovit zu Biotit praktisch nur druckabhängig.

tion has therefore to be treated with care. We are currently investigating this observation in more detail.

The fact that the Plattengneiss contains a variety of minerals with different rheological behaviour offers a good possibility to explore the parameter space of exponential flow laws in order to constrain the stresses which are responsible for the formation of the observed textures. For garnet no experimental data are available, therefore we use the experimentally well-constrained minerals quartz and feldspar and model a situation where quartz becomes harder than feldspar as an upper limit of the parameter space. We call this extraordinary rheological situation strength reversal and try to get on this way information on the limiting parameters of the stress evolution of the Plattengneiss.

4. Strength reversal

In order to explore the stresses and physical conditions at which quartz may be the strongest phase in polyphase rocks we assume that all minerals in the Plattengneiss are deformed according to a non-linear viscous constitutive relationship where stress raised to some power is proportional to strain rate and inverse exponentially related to temperature. These relations are well known as the “power law” and “Arrhenius” relationship, respectively and commonly written in the form:

$$\Delta\sigma = \left(\frac{\dot{\epsilon}}{A}\right)^{\frac{1}{n}} \exp\left(\frac{Q}{nRT}\right) \quad (1)$$

where $\Delta\sigma$, is the differential stress in [M Pa], $\dot{\epsilon}$ is strain rate in [s^{-1}], A is a pre exponent constant in [$Pa^{-n}s^{-1}$], Q is the activation energy in [$Jmol^{-1}$], R is the gas constant in [$Jmol^{-1}^{\circ}K^{-1}$] n is the stress exponent and T is absolute temperature in [$^{\circ}K$]. According to ENGLAND & MCKENZIE (1982) all material constants and temperature dependent parts of eq. (1) may be combined to a constant B ($[Pa s^{-n}]$) so that:

$$B = A^{-\frac{1}{n}} \exp\left(\frac{Q}{nRT}\right) \quad (2)$$

Equation (1) simplifies therefore and can be written as:

$$\Delta\sigma = B \dot{\epsilon}^{\frac{1}{n}} \quad (3)$$

When temperature trends to infinite and stress exponent goes to 1 eq. (1) reduces to a linear proportionality between stress and strain rate. This is called a “Newtonian fluid” and the proportionality constant is called viscosity and has the dimensions of [$Pa s$]. The term “viscosity” cannot be used in power law. However, it is possible to define an “effective viscosity” $\eta_{(eff)}$ as a ratio of stress to strain rate.

$$\eta_{(eff)} = \frac{\Delta\sigma}{\dot{\epsilon}} = \frac{B \dot{\epsilon}^{\frac{1}{n}}}{\Delta\sigma^n B^{-n}} = B \dot{\epsilon}^{\left(\frac{1}{n}-1\right)} \quad (4)$$

The relation between differential stress and strain rate described by eq.(4) is illustrated for two relevant mineral phases on (Fig. 3a). As an example we plotted the curves for quartz and albite (data are listed in Table 1) for a temperature of $500^{\circ}C$. The two curves show the non-linear dependence of strain rate on differential stress at power law deformation. The slope of the curve is defined by the “effective viscosity” and the curvature is related to n . The simple direct proportionality of eq. (4) is only true for the one dimensional case. For the general case (co-ordinate independent calculations) $\dot{\epsilon}$ must be replaced by the second invariant of the strain rate tensor E . However, here we consider only the one dimensional case and use eq.(1).

4.1 Conditions for strength reversal

In the next section we describe the conditions that are necessary for strength reversal according to power law rheology. This is given when:

$$SC = \frac{\Delta\sigma_m}{\Delta\sigma_q} = \frac{\eta_{(eff)m}}{\eta_{(eff)q}} = 1 \quad (5)$$

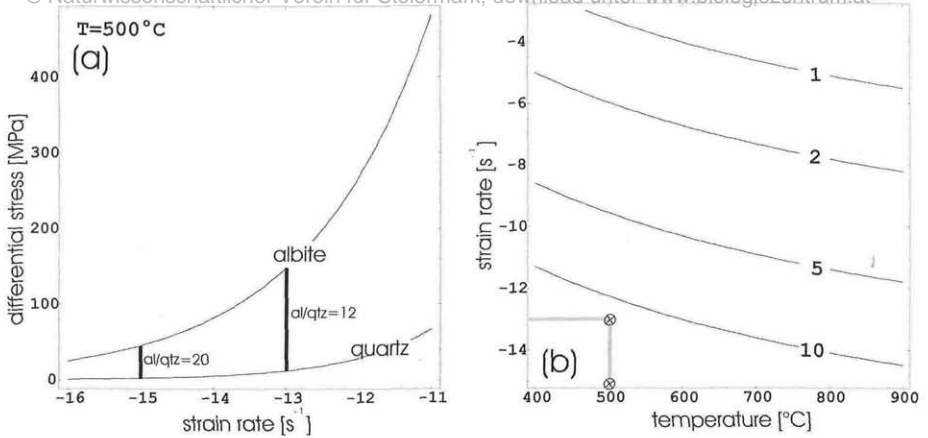


Fig. 3: (a) Differential stress versus logarithmic strain rate for two minerals (quartz and albite) using the available data of CARTER & TSENN (1986) at constant temperature of 500° C. (b) “Effective viscosity contrast” of quartz and albite in a given range of strain rate against temperature. The “1”-contour indicates the so called strength reversal. “x” marks geological relevant conditions which are comparable to the bars in (a).

(a) Differenzialspannung gegen logarithmische Verformungsrate für zwei Minerale (Quarz und Albit) unter Verwendung der experimentellen Daten von CARTER & TSENN (1986) bei konstanter Temperatur von 500° C. (b) “Effektiver Viskositätskontrast” von Quarz und Albit in einem gewählten Bereich von Verformungsrate und Temperatur. Die “1”-Kontur bezeichnet die sogenannte Festigkeitsumkehr. “x” bezeichnet geologisch relevante Bedingungen, die vergleichbar sind zu den Balken in (a).

A strength contrast (SC) of 1 indicates that both minerals have the same strength whereas 10 means that albite is ten times “harder” than quartz.

In eq. (5), and therefore in the experimentally derived eq. (1), three constants play an important role, the relative activation energies, the relative pre exponent constants and the relative stress exponents. We took the constants of BRACE & KOHLSTEDT (1980) and CARTER & TSENN (1987) and varied all the parameters.

Reconsidering (Fig. 3) it can be seen that in the shown range of strain rates quartz is rheologically weaker than albite. At a strain rate of $10^{-13} [s^{-1}]$ the SC ratio between albite and quartz is about 12. At a strain rate of $10^{-15} [s^{-1}]$ the SC ratio increases to a value around 20 which means that albite is 20 times harder than quartz, if both minerals deform at this strain rate. In (Fig. 3b) we show a generalisation of (Fig. 3a). It may be seen that the strength contrast between albite and quartz decreases with increasing temperature and increasing strain rate. It may also be seen that albite becomes stronger than quartz only at geologically irrelevant strain rates above $\dot{\epsilon}=10^{-5} [s^{-1}]$ and temperatures above 700° C. Assuming strength reversal ($SC=1$) as an upper limit in Plattengneiss rocks (Fig. 1) we can conclude that albite data combined with quartz porphyroclasts are unrealistic to describe this certain material behaviour of the assumed rheology. This is no surprise because there are no exact power law constants available for the feldspar of the Plattengneiss and it must also be taken into account that the Plattengneiss matrix is polyphase and aggregates of quartz and feldspar behave in a different way to experimentally derived data of monomineralic aggregates. We know the temperature ranges for the Plattengneiss around (600° C to 700° C) and geologically relevant strain rates in the ductile regime are unlikely to be greater than $10^{-12} [s^{-1}]$ to $10^{-13} [s^{-1}]$. We can therefore proceed to use this range of known physical conditions to extract the material constants relevant for the Plattengneiss.

4.2 Parameter space for strength reversal:

The last section has shown – using the experimental data for quartz and feldspar – quartz can only be stronger than feldspar at unrealistic strain rates. But we want to find out the limiting values for the rheology of quartz and feldspar aggregates. Therefore we now reverse our logic and explore the material constants $A_{(m)}$, $Q_{(m)}$ and $n_{(m)}$ that are needed relative to quartz to allow strength reversal at realistic strain rates and temperatures. We took quartz data of CARTER & TSENN (1987) for default values and calculated strength reversal for ranges of pre exponent constants and activation energies and stress exponents. The temperature for strength reversal is given by solving eq.(5) for temperature:

$$T_{(rev)} = \frac{Q_m n_q - Q_q n_m}{n_q n_m} \ln \left(\frac{\frac{1}{A_m} \frac{1}{\dot{\epsilon}}^{\frac{1}{n_m}}}{\frac{1}{A_q} \frac{1}{\dot{\epsilon}}^{\frac{1}{n_m}}} \right)^{-1} \quad (6)$$

In a similar way the strain rates for strength reversal for a given range of $Q_{(m)}$ and $A_{(m)}$ data can be derived:

$$\dot{\epsilon}_{(rev)} = \left(A_m^{-\frac{1}{n_m}} A_q^{\frac{1}{n_q}} \exp \left(\frac{Q_m}{n_m RT} - \frac{Q_q}{n_q RT} \right) \right)^{\left(\frac{n_m n_q}{n_m - n_q} \right)} \quad (7)$$

Eq. (6) shows that strength reversal is temperature independent when $Q_{(m)} = n_{(m)} / n_{(q)} Q_{(q)}$. Eq. (7) shows that strength reversal occurs at infinite strain rates when $n_{(m)} \rightarrow n_{(q)}$. In (Fig. 4) we plotted the strain rates needed for strength reversal between matrix and quartz calculated with eq.(7), that occurs as a function of the matrix material constants $Q_{(m)}$, $A_{(m)}$ and $n_{(m)}$. The contours show a geologically relevant range of strain rates between 10^{-10} [s^{-1}] and 10^{-16} [s^{-1}].

In (Fig. 4a) we assumed a temperature of 500° C and a stress exponent of $n_{(m)}=2$. We included the position of several minerals in a $Q_{(m)}$ - $A_{(m)}$ -field although some of these experimental data are not related to $n_{(m)}=2$ for these minerals. So the contoured lines are only valid strength reversal strain rates of quartz coexisting with a hypothetical mineral of the stress exponent $n_{(m)}=2$. In (Fig. 4) we varied two things. On the one hand the temperature and on the other hand the stress exponent. It can be clearly seen on (Fig. 4a-d) that a variation of temperature is not as effective as a variation of stress exponent on the evolution of the strain rate curves for strength reversal. Another important point is the relation of the stress exponent of the investigated mineral phase to the coexisting dry quartz. As we know dry quartz has a stress exponent $n_{(q)}=2.72$. A smaller value of $n_{(m)}=2$, leads to decreasing strain rates with increasing activation energy $Q_{(m)}$. If $n_{(m)}=3$ (higher than $n_{(q)}$ of dry quartz) exactly the opposite is the case. Strain rates of reversal increase with increasing activation energy. If the stress exponent of both minerals is equal, all strain rate curves would plot at the same position. Then, strength reversal is independent on strain rate. Remembering (Fig. 3) we got a strength reversal for quartz and albite at very fast strain rates and high temperatures and asked about the conditions of geological relevant strength reversal. Now we can assume that the higher the contrast of both stress exponents between two coexisting minerals, the more probable a strength reversal can appear during geologically relevant conditions of deformation.

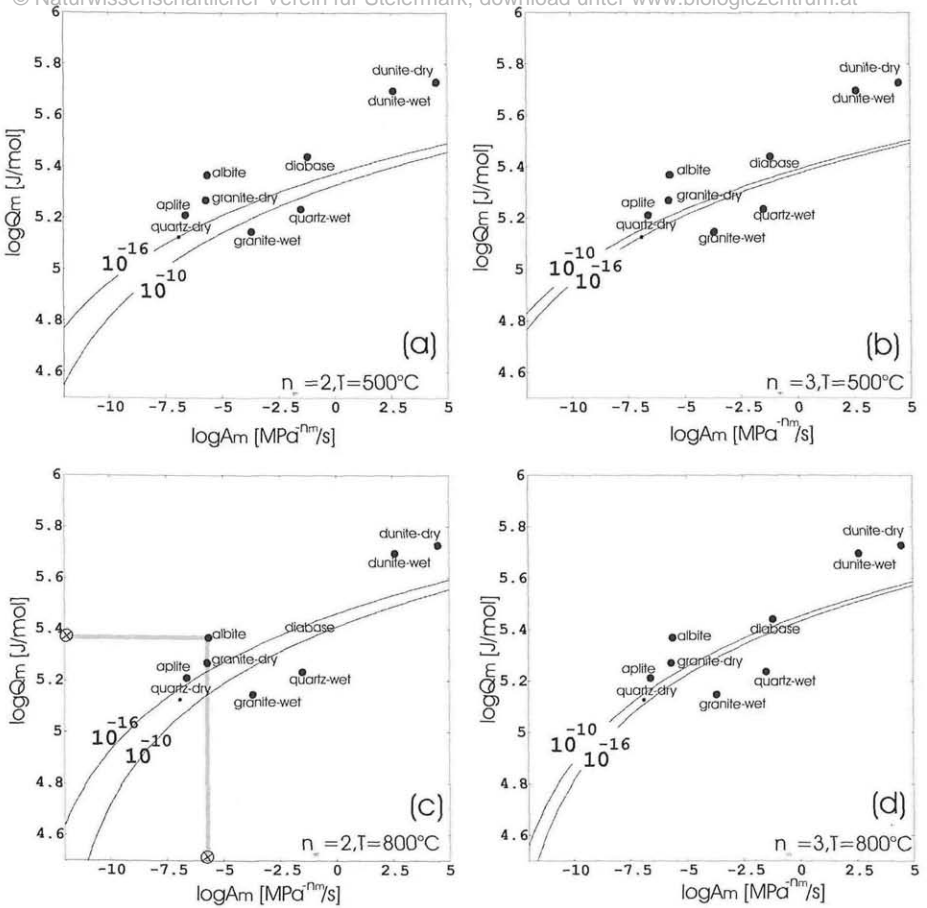


Fig. 4: Logarithmic $Q_{(m)}$ - $A_{(m)}$ -diagrams with strain rate contours of strength reversal for different stress exponents and temperatures. Minerals are plotted as points in the $Q_{(m)}$ - $A_{(m)}$ -field, not corresponding to the assumed stress exponent.

Logarithmische $Q_{(m)}$ - $A_{(m)}$ -Diagramme mit konturierten Verformungsraten für Festigkeitsumkehr für verschiedene Spannungsexponenten des Potenzgesetzes und Temperaturen. Minerale sind als Punkte im $Q_{(m)}$ - $A_{(m)}$ -Feld geplottet, und entsprechen nicht dem gewählten Spannungsexponenten.

In Table (1) the used data from literature are shown and also the resulting strain rates and differential stress, we calculated for strength reversal. In these data too fast strain rates and corresponding differential stress occur for strength reversal. Therefore these calculations are not useful for interpreting the strength reversal conditions. We only can predict approximately the range of $Q_{(m)}$ and $A_{(m)}$ -values for polyphase aggregates.

Table(1): Flow law parameters for certain minerals; $\dot{\epsilon}_m$ is strain rate for strength reversal and $\Delta\sigma_{(rev)}$ is differential stress for strength reversal (experimentally derived data of CARTER & TSENN 1987)

Parameter	quartz-dry	quartz-wet	albite	granite-wet	granite-dry	aplite
A [$\text{Pa}^{-n}\text{s}^{-1}$]	$10^{-6.9}$	$10^{-1.5}$	$10^{-3.63}$	$10^{-3.7}$	$10^{-3.7}$	$10^{-6.6}$
Q [Jmol^{-1}]	134000	172000	234200	140600	186500	163200
n	2.72	1.9	3.9	1.9	3.3	3.1
$\dot{\epsilon}_{(rev)}$ [s^{-1}]		$2.4 \cdot 10^{-5}$	$3.2 \cdot 10^{-7}$	$2.2 \cdot 10^{-5}$	$9.6 \cdot 10^{-6}$	$1.1 \cdot 10^{-3}$
$\Delta\sigma_{(rev)}$ [MPa]		12481.8	3052.73	2952.05	620.707	2177.01

Eq.(5) can also be solved for the stress exponent of the matrix necessary for the strength reversal to occur at reasonable strain rates.

This is given by

$$n_m(rev) = y \log(x)^{-1} \quad (8)$$

where

$$x = \left(\frac{\dot{\epsilon}}{A_q} \right)^{\frac{1}{n_q}} \exp\left(\frac{Q}{n_q RT} \right) \quad \text{and} \quad y = \left(\frac{\dot{\epsilon}}{A_m} \right) \exp\left(\frac{Q}{RT} \right) \quad (9)$$

Using eq.(8) we calculated the stress exponents for strength reversal assuming geologically reasonable strain rates of 10^{-13} [s^{-1}] and 10^{-16} [s^{-1}] and temperatures of 500°C and 800°C . The stress exponent is one of the most important material parameters responsible for the relative rheological behaviour of different mineral phases. The resulting values (Table 2 and 3) for $n_m(rev)$ show a wide range but can be used as a good estimate for stress exponent of polyphase aggregates at these assumed conditions.

Table (2) shows calculated stress exponent $n_m(rev)$ for strength reversal for two different temperatures (500°C and 800°C) at a given strain rate of 10^{-13} [s^{-1}].

Table(2)	$T=500^\circ\text{C}$	$T=800^\circ\text{C}$
$n(\text{granite-dry})$	4.81	11.37
$n(\text{granite-wet})$	0.12	15.6
$n(\text{aplite})$	4.26	9.87
$n(\text{albite})$	7.77	25.14
$n(\text{quartz-dry})$	0.11	-19.91

Table(3)	$T=500^{\circ} C$	$T=800^{\circ} C$
$n_{(granite-dry)}$	-155.43	1.28
$n_{(granite-wet)}$	188.1	5.16
$n_{(aplite)}$	-109.92	1.5
$n_{(albite)}$	-367.79	-1.09
$n_{(quartz-dry)}$	193.27	6.47

5. Conclusions

Assuming that the deformation of the Plattengneiss can be described by power law relationship where stress is proportional to the n-th power of strain rate we come to the following results:

1. The observation that the Plattengneiss contains different rigid minerals, e.g. feldspar, garnet and quartz-feldspar aggregates in a weaker matrix cannot be explained with experimental data for single phase aggregates. Our results represent the so called strength reversal for quartz and feldspar as an upper limit for the rheology of the multiphase quartz-feldspar rocks of the Plattengneiss shear zone. Assuming geologically relevant strain rates and temperatures the variation of the stress exponent using experimentally derived constants for activation energy is considerably high, e.g. the stress exponent for albite at relevant strain rates ranges between -1.09 and 25.14 for an assumed temperature of 800°C. The stress exponent in power law plays an important role during ductile deformation. The more precise the parameters of the flow law can be constrained the better the solution for the stress exponent. Based on the maximum constraints of strength reversal for quartz and feldspar, this method can be used for several mineral assemblages, e.g. the pegmatitic layers in the Plattengneiss can be compared with aplite rheology with a stress exponent ranging between 1.5 and 9.87 for the conditions mentioned above.

2. The fact that biotite grows in pressure shadows around garnets on the expense of muscovite is generally interpreted as a decompression reaction due to exhumation. We show that a local decrease of mean stress (e.g. in a pressure shadow) of 100 MPa can change the volumetric proportions of biotite, muscovite and garnet by roughly the same amount as is observed in the Plattengneiss rocks. As 100 MPa is a realistic magnitude for differential stress contribution to mean stress, we suggest that this observation implies that care must be taken in the interpretation of decompression textures as indicators for exhumation.

These considerations serve as a basic approach for understanding the complex rheological relationship in polyphase rocks and a help in constraining the dynamic parameters responsible for the creation of the Plattengneiss shear zone.

References

- BRACE W.F., KOHLSTEDT D.L. 1980: Limits on Lithospheric Stress Imposed by Laboratory Experiments. – Journal of Geophysical Research 85/11: 6248-6252.
 CARTER N.L., TSENN M.C. 1987: Flow properties of continental lithosphere. – Tectonophysics 156: 27-63.

- ENGLAND P., MCKENZIE D. 1982: A thin viscous sheet model for continental deformation. – *Geophys. J. R. astr. Soc.* 70: 295–321.
- ERNST W.G. 1971: Do mineral parageneses reflect unusually high pressure conditions of Franciscan metamorphism? – *American Journal of Science* 270: 81–108.
- FLÖTTMANN T., KLEINSCHMIDT G., WOLF D. 1986: Deformationsanalyse der unteren Gneisgruppe in der südlichen Koralpe (Ostalpen). – *Carinthia II* 176/96: 179–202.
- KROHE A. 1987: Kinematics of Cretaceous nappe tectonics in the Austroalpine basement of the Koralpe region (eastern Austria). – *Tectonophysics* 136: 171–196.
- MANCKTELOW N.S. 1993: Tectonic overpressure in competent mafic layers and the development of isolated eclogites. – *Journal of metamorphic Geology* 11: 801–812.
- MILLER C. 1990: Petrology of the type locality eclogites from the Koralpe and Saualpe (Eastern Alps), Austria. – *Schweiz. Min. Pet. Mitt.* 70: 287–300.
- MILLER C., FRANK W. 1983: Das Alter der Metamorphose von Metabasiten und Eklogiten in Kor- und Saualpe. – In: *Die frühalpene Geschichte der Ostalpen. Jahresber. Hochschulschwerpunkt S* 15/4: 229–236.
- MOLNAR P., LYON-CAEN H. 1988: Some simple physical aspects of the support, structure, and evolution of mountain belts. – *Geological Society of America, Special Paper* 218: 179–207.
- MOLNAR P., ENGLAND P. 1990: Temperatures, Heat Flux, and Frictional Stress Near Major Thrust Faults. – *Journal of Geophysical Research* 95/4: 4833–4856.
- NEUBAUER F., DALLMEYER R.D., DUNKL I., SCHIRNIK D. 1995: Late Cretaceous exhumation on the metamorphic Gneissalpe dome, Eastern Alps: Kinematics, cooling history and sedimentary response in a sinistral wrench corridor. – *Tectonophysics* 242: 79–98.
- RUTLAND R.W.R. 1965: Tectonic overpressures. – In: PITCHER W.S., FLINN G.W. (Eds.): *Controls of Metamorphism* 119–139. – Edinburgh, Verl. Oliver & Boyd.
- SHELTON G.L., TULLIS J. 1981: Experimental flow laws for crustal rocks. – *EOS, Trans. Am Geophys. Union* 62: 396.
- SONDER L.J., ENGLAND P. 1986: Vertical averages of rheology of the continental lithosphere: relation to thin sheet parameters. – *Earth and Planetary Science Letters* 77: 81–90.
- STÜWE K. 1998: Heat sources of Cretaceous metamorphism in the Eastern Alps – a discussion. – *Tectonophysics* 287: 251–269.
- STÜWE K., POWELL R. 1995: PT paths from modal proportions. Applications to the Koralm Complex, Eastern Alps. – *Contributions to Mineralogy and Petrology* 119: 83–93.
- THÖNI M., JAGOUTZ E. 1992: Some new aspects of dating eclogites in orogenic belts: Sm-, Nd, Rb-Sr and Pb-Pb isotopic results from the Austroalpine Saualpe and Koralpe type locality (Carinthia/Styria, southeastern Austria). – *Geochimica et Cosmochimica Acta*: 347–368.
- THÖNI M., MILLER C. 1996: Garnet Sm-Nd data from the Saualpe and the Koralpe (Eastern Alps, Austria): chronological and PT constraints on the thermal and tectonic history. – *Journal of Metamorphic Geology* 14: 453–466.